AIP | The Journal of Chemical Physics

On the calculation of solubilities via direct coexistence simulations: Investigation of NaCl aqueous solutions and Lennard-Jones binary mixtures

J. R. Espinosa, J. M. Young, H. Jiang, D. Gupta, C. Vega, E. Sanz, P. G. Debenedetti, and A. Z. Panagiotopoulos

Citation: The Journal of Chemical Physics **145**, 154111 (2016); doi: 10.1063/1.4964725
View online: http://dx.doi.org/10.1063/1.4964725
View Table of Contents: http://scitation.aip.org/content/aip/journal/jcp/145/15?ver=pdfcov
Published by the AIP Publishing

On the calculation of solubilities via direct coexistence simulations: Investigation of NaCl aqueous solutions and Lennard-Jones binary mixtures

J. R. Espinosa,[1] J. M. Young,[2] H. Jiang,[2] D. Gupta,[2] C. Vega,[1] E. Sanz,[1]
P. G. Debenedetti,[2] and A. Z. Panagiotopoulos[2,a)]
[1]*Departamento de Quimica Fisica I, Facultad de Ciencias Quimicas, Universidad Complutense de Madrid, 28040 Madrid, Spain*
[2]*Department of Chemical and Biological Engineering, Princeton University, Princeton, New Jersey 08544, USA*

(Received 11 August 2016; accepted 29 September 2016; published online 19 October 2016)

Direct coexistence molecular dynamics simulations of NaCl solutions and Lennard-Jones binary mixtures were performed to explore the origin of reported discrepancies between solubilities obtained by direct interfacial simulations and values obtained from the chemical potentials of the crystal and solution phases. We find that the key cause of these discrepancies is the use of crystal slabs of insufficient width to eliminate finite-size effects. We observe that for NaCl crystal slabs thicker than 4 nm (in the direction perpendicular to the interface), the same solubility values are obtained from the direct coexistence and chemical potential routes, namely, 3.7 ± 0.2 molal at T = 298.15 K and p = 1 bar for the JC-SPC/E model. Such finite-size effects are absent in the Lennard-Jones system and are likely caused by surface dipoles present in the salt crystals. We confirmed that μs-long molecular dynamics runs are required to obtain reliable solubility values from direct coexistence calculations, provided that the initial solution conditions are near the equilibrium solubility values; even longer runs are needed for equilibration of significantly different concentrations. We do not observe any effects of the exposed crystal face on the solubility values or equilibration times. For both the NaCl and Lennard-Jones systems, the use of a spherical crystallite embedded in the solution leads to significantly higher apparent solubility values relative to the flat-interface direct coexistence calculations and the chemical potential values. Our results have broad implications for the determination of solubilities of molecular models of ionic systems. *Published by AIP Publishing.* [http://dx.doi.org/10.1063/1.4964725]

I. INTRODUCTION

Sodium chloride in water is arguably the most important aqueous solution in nature because of its high relevance in environmental, geochemical, industrial, and biological systems. For this reason, numerous experimental, theoretical, and computational studies have been devoted to electrolyte solutions, especially aqueous NaCl solutions.[1–5] In recent years, there has been increasing interest in the development of accurate molecular-based models for the properties of electrolyte solutions[6–10] (see the work of Nezbeda *et al.*[11] for a recent review). One of the important properties of such solutions is the solubility of the salt in water. The experimental solubility for sodium chloride in water at 298.15 K and 1 bar is 6.14m[12] (moles of salt per kilogram of water, denoted as molality (m)), but most force fields[6–10] underestimate this quantity. Available algorithms for solubility calculations can be divided into two main categories. The first is the chemical potential route (CPR) where the solubility is determined as the salt concentration at which the electrolyte chemical potential is equal to that of the crystal solid. The second is the direct coexistence method (DCM) in which a solution is placed in contact with a crystalline slab of salt, and the solubility is obtained by measuring the concentration of the solution after the system has reached equilibrium.

Even though DCM simulations have been widely used in the past,[13–15] and their agreement with free energy based calculations has been demonstrated for many systems,[16–20] there are significant unresolved discrepancies between DCM and CPR for calculating the solubility of NaCl in water.[11] The solubility obtained by DCM is generally higher than the corresponding value obtained by CPR, and different implementations of DCM yield different values for the solubility,[21–24] while multiple groups have obtained similar values for the solubility of NaCl in water using CPR.[9,25–32] To cite a specific example, the solubility of the Joung-Cheatham NaCl model in SPC/E water (JC-SPC/E)[6,33] at 298.15 K and atmospheric pressure is 3.7m ± 0.2m, as reported from independent CPR calculations by different groups,[25,27,28,32] while the solubility of the same model obtained by the DCM approach ranges from 5.5m to 8.1m.[21–24]

The main aim of the present work is to understand the origin of such discrepancies between the DCM and CPR approaches and thereby to determine a reliable methodology to obtain salt solubilities. We choose to use the JC-SPC/E[6,33] force fields since the solubility of the model has been well established by CPR calculations, as stated in the previous

a)Author to whom correspondence should be addressed. Electronic mail: azp@princeton.edu

paragraph. We find that the fundamental causes of these discrepancies are finite-size effects and slow equilibration of the solution in the presence of a salt crystal. Finite-size effects on the calculation of salt solubility were observed previously by Kobayashi *et al.*[22] who found that the solubility of NaCl decreased from 8.1m to 6.2m when the number of ions in the crystal increased from 512 to 1000. To understand the origin of the strong finite size effect in solubility calculations using DCM, we also investigated the solubility of a binary Lennard-Jones (LJ) mixture without charge.[34]

Finally, we performed a different variant of DCM[23,24] to estimate the solubility, consisting of inserting a spherical crystal seed into the solution. Our simulations show that for both systems (NaCl solution and LJ mixture), this approach overestimates solubility even when a large crystal seed is used.

II. MODELS AND SIMULATION DETAILS

For the system of NaCl and water, the ions were modeled with the Joung-Cheatham force field,[6] which consists of 12-6 LJ potentials plus Coulombic interactions, and the water molecules were represented by the SPC/E model.[33] The LJ mixture was composed of a model solute (S) and solvent (SV) with the same diameter but different interaction energy.[34] The cross interactions between solute and solvent particles control the solubility and cause steric hindrance between the solute and solvent that prevents solvent from entering the crystal. The parameters of the force fields studied in this work are given in Table I.

Molecular dynamics simulations were performed using the GROMACS[35] package for both the NaCl-water and the binary LJ systems. For the simulation of the NaCl-water system using the JC-SPC/E force fields, all runs were performed at a constant pressure of 1 bar and at a temperature of 298.15 K. Direct coexistence simulations were performed in the NpT ensemble using an anisotropic Parrinello-Rahman barostat[36] with a relaxation time of 1 ps and a Nosé-Hoover[37] thermostat with a relaxation time of 0.5 ps. The time step for the Verlet integration of the equations of motion was 2 fs. We used particle mesh Ewald summations[38] to deal with the electrostatic interactions. The cutoff radius for both dispersive interactions and the real part of the electrostatic interactions was 9 Å. Long range LJ corrections were included. The LINCS algorithm[39] was used for constraining the O–H bond length in water.

TABLE I. Parameters for the JC-SPC/E and LJ binary force fields. The cross interactions for the JC-SPC/E model have been obtained by the Lorentz-Berthelot combining rules.

Model	LJ interaction	ϵ/k_B (K)	σ (Å)	Charge	q (e)
SPC/E	O–O	78.20	3.166	O	−0.8476
SPC/E				H	0.4238
JC	Na^+–Na^+	177.457	2.159	Na^+	+1.0
JC	Cl^-–Cl^-	6.434	4.830	Cl^-	−1.0
JC	Na^+–Cl^-	33.789	3.495		
JC	Na^+–O	117.841	2.663		
JC	Cl^-–O	22.430	3.998		
LJ	S-S	114.128	3.405		
LJ	SV-SV	61.691	3.405		
LJ	S-SV	74.406	3.798		

For direct coexistence simulation of salt solubility in water, a block of the salt crystalline solid was introduced on one side of the simulation box, and water (or aqueous solution) was introduced on the other side. The NaCl planes in contact with the solution were modified adding some defects (e.g., removing some of the ions) to accelerate the kinetics of the ion exchange between the solution and the slab. After the system reached equilibrium, generally after several hundred nanoseconds (depending on system size), the solubility was estimated as the concentration of NaCl in solution. We used two different criteria to determine the concentration of our solutions: a "qualitative criterion" to evaluate the trend of the concentration as a function of time and a "quantitative criterion" to obtain the exact solubility after the system reached equilibrium. The "qualitative criterion" measures the number of ions in the crystal slab ($N_{Solid,ions}$) which is subtracted from the total number of ions to obtain the number of ions in the solution. The concentration is then computed by

$$m_{\mathrm{NaCl},approx} = \frac{N_{Total,ions} - N_{Solid,ions}}{2M_w N_w}, \tag{1}$$

where the division by 2 accounts for a pair of ions, M_w = 0.018 015 kg/mol, and N_w is the number of water molecules of the system. In order to identify the ions that belong to the crystal slab, we used the local bond order parameter introduced by ten Wolde *et al.*[40] The definition used for labeling an ion as "solid-like" is the same as in Refs. 41 and 42 with the exception that an ion is considered solid when at least 4 neighboring ions have a scalar product $q_4(i) \cdot q_4^*(j)$ larger than 0.35, instead of the 6 neighbor ions used in Refs. 41 and 42 (for more details see the Appendix of Ref. 41). The reason for this tuning is that we obtained better (almost quantitative) agreement of this local order parameter with the density profile, as can be seen in Fig. 1. The density profile ("the quantitative criterion") determines the solubility from the partial mass density of water and ions in the bulk of the solution, marked in Figure 1(a) by two vertical dashed lines, using

$$m_{\mathrm{NaCl}} = \frac{\rho_z^{ions}}{\rho_z^{\mathrm{H_2O}} M_s}, \tag{2}$$

where ρ_z^{ions} stands for the mass density of ions, $\rho_z^{\mathrm{H_2O}}$ is the mass density of water, and M_s = 0.058 44 kg/mol is the molar mass of the salt. The density profiles were calculated using the GROMACS tool[35] "g_density" and were evaluated over the period of time during which the systems were completely equilibrated.

In summary, the approach that we followed to obtain the salt solubilities from DCM was to first monitor the concentration in the solution as a function of time using the q_4 parameter, and when the system has reached equilibrium (300 ns in this case, as shown in Fig. 1(b)), to evaluate the density profile.

For the LJ binary mixture, the simulations were also performed in the NpT ensemble using the Nosé-Hoover thermostat[37] with a relaxation time of 1 ps. A Parrinello-Rahman[36] barostat was used, isotropic for the thermodynamic

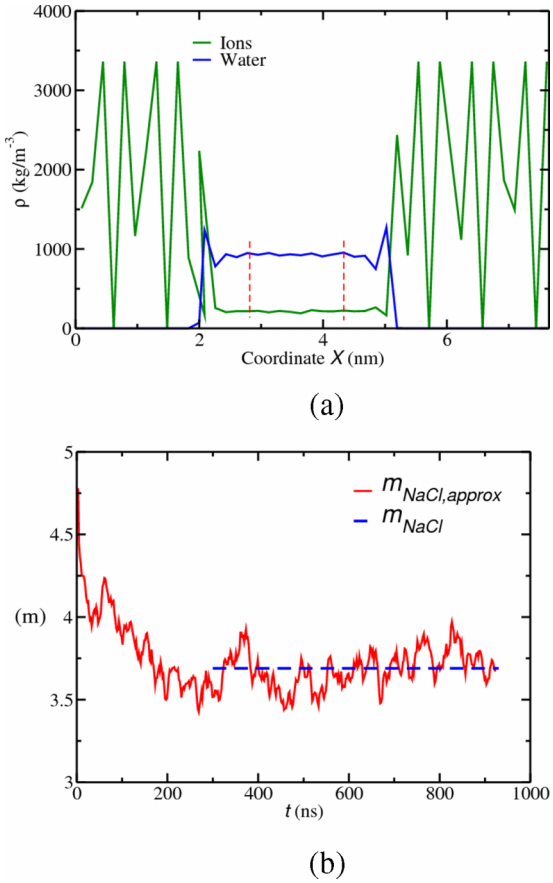

FIG. 1. Both panels correspond to a system composed of 2830 ions in a crystal slab in contact with a solution of 1620 molecules of water with an initial salt concentration of about $4.75m$. The crystal orientation exposed at the interface was the (100) face. (a) Density profile for the ions (green curve) and for water (blue curve) obtained once the system reached equilibrium (after 300 ns, see (b)). Vertical red dashed lines indicate the region of the computational cell that we have used to estimate the solution concentration. Notice that the crystal solid slab in our simulations has been split into two in the figure due to the periodic boundary conditions. (b) Solubility (red curve) as a function of time, measured using the q_4 local order parameter. The dashed blue line represents the value of solubility averaged after equilibration ($t > 300$ ns) using the density profile criterion.

integration simulations and anisotropic for the direct coexistence ones with a relaxation time in both cases of 2 ps. The time step was set to 1 fs using the Leap-frog algorithm.[43] The potential was cut and shifted at 2.5 σ (8.5125 Å) and no long-range corrections were used. The mass for particles (both S and SV) was the one of argon (0.039 948 kg/mol). All simulations were performed at 50 K and 1 bar. The solubility was determined by counting the number of solute and solvent particles in the bulk region of the liquid in a similar fashion as for the calculations of NaCl solubility.

III. DIRECT COEXISTENCE SIMULATION FOR NaCl SOLUBILITY IN WATER

In the following, we address how the solubility calculated from direct coexistence simulations depends on system size and geometry, the crystal orientation exposed to the interface, and the initial concentration of the solution in contact with the crystal slab.

A. Finite size effects on solubility estimation

We first studied the effects of system size and geometry of the crystal slab on the solubility. We performed simulations with different numbers of ions in the crystal slab, numbers of water molecules, widths of the crystal slab, and interfacial areas. The size parameters and solubilities of the systems studied are given in Table II. For each system, we launched 5 independent simulations with different initial momenta. It is clear that solubility depends on the system used in each case, but the question is the following: what variable causes the change in solubility from one system to another?

As shown in Table II, cases A and B both have a crystal slab width (in the direction perpendicular to the solid-solution interface) of 2.1 nm and the same calculated solubility (about $5.7m$) even though case B has more ions in the crystal and a correspondingly larger interfacial area. Therefore, it can be concluded that the solubility does not depend solely on the number of the ions in the crystal or on the area of the crystal-solution interfaces. Cases C and D have a similar crystal width (about 3 nm) but case D has more ions in the crystal and more water in the solution. Since both cases yield a similar solubility, simply enlarging the system size may not necessarily yield better agreement with CPR calculations. For cases E, F and G, the width of the crystal slab is larger, and we obtained solubility values consistent with CPR calculations and significantly lower than in cases A-D. In Fig. 2, we plot the solubility as a function of the inverse width of the crystal slab, and it is clear that the solubility calculated from the DCM converges to the values obtained by CPR calculation as the crystal width increases. Previous studies[21,23] in which the width of the crystal slab was smaller than the values used here reported higher values of solubility, which are in agreement with the ones estimated in this work for smaller crystal slab widths (cases A, B, C, and D).

B. Statistical noise aspects of direct coexistence simulations

A stochastic event, such as nucleation,[44,45] is an unpredictable phenomenon due to the influence of random fluctuations. In the case of direct coexistence simulations, stochasticity has been studied previously when determining

TABLE II. The number of ions in the crystalline slab N_{ions}, the number of water molecules in the solution N_{water}, the width of the ionic crystal slab L_{slab}, the area of the interface A_{int}, and the solubility m_{NaCl} obtained from the density profile criterion once systems had reached equilibrium. The number in parenthesis indicates the error of our solubility estimates. For all systems the initial concentration of the solution was about $4m$ and the (100) crystal face was exposed to the interface.

Name	N_{ions}	N_{water}	L_{slab} (nm)	A_{int} (nm^2)	m_{NaCl}
A	512	810	2.1	5.4	5.7(4)
B	1568	810	2.1	16.4	5.6(4)
C	1000	1620	2.9	8.4	5.3(4)
D	4000	6480	3.0	33.5	5.1(4)
E	2830	1620	4.0	17.4	3.5(4)
F	3136	1620	4.7	16.4	3.8(4)
G	8192	6480	10.0	21.3	3.9(4)

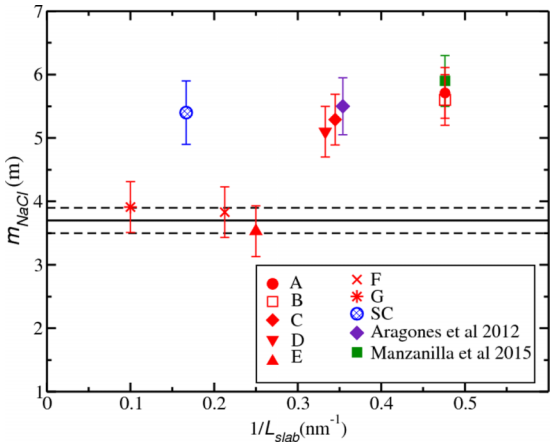

FIG. 2. NaCl solubility for all system sizes studied as a function of the inverse width of the crystal slab. Red symbols are our results for direct coexistence simulations, black lines indicate the value and error obtained by chemical potential simulations (CPR),[25,27,28] the green square[23] and purple diamond[21] denote the previous literature results using direct coexistence simulations. Error bars were estimated at $0.4m$ due to statistical noise between runs of about $0.3m$ (see Fig. 3 and Section III B) and an uncertainty in the density profile of $0.1m$. The spherical crystallite (SC) value (explained in Sec. V and the supplementary material) has been plotted taking the inverse of its diameter (1/D) as the characteristic dimension.

the coexistence pressure[13] of a pseudo-hard-sphere potential.[46] However, direct coexistence simulations for estimating solubilities are not affected by stochasticity in principle, since the system only has two components and it will evolve to equilibrium irrespective of the initial momenta when the simulated time tends to infinite. Although stochasticity indeed plays a role in the time needed for a given initial configuration to reach its equilibrium state, this effect becomes more pronounced when the initial solution concentration is further from the solubility. In order to reduce the error in our solubility estimations, we have performed 5 independent runs for every case starting from the same initial configuration but with different initial velocities. The temporal evolution of salt concentration for five independent case E trajectories is shown in Fig. 3. When the initial velocities of molecules in an initial configuration were changed, the trajectories can be different until equilibrium is reached (e.g., maroon compared to green trajectory). However after equilibrium is reached, the concentrations fluctuate around the equilibrium value regardless of the initial momenta. These fluctuations, as shown in Fig. 3, introduce statistical noise which results in additional uncertainty of about $0.3m$ in the solubility for runs of 1 μs duration in the NaCl system. This uncertainty can be reduced by running more simulations, using longer simulation times, or by enlarging the system size (e.g., 10 000 ions in the crystal slab); however, all of these strategies result in a higher computational cost.

C. Dependence on the crystal face exposed to the interface

The next question addressed is the dependence of solubility on crystal orientation. Kolafa presented results of DCM calculations for this same model in a conference in 2015,[47] observing that crystal planes with high Miller indices lead to lower solubility values that were in good agreement with results estimated by CPR.[25,27,28] It is possible that some crystal planes have lower activation energies associated with dissolution into an unsaturated solution or growth into a supersaturated one; however, solubility should — in principle — be the same regardless of the plane exposed to the solid-solution interface, even though the equilibration time of simulations could be different. To understand the effect of crystal orientation on solubility, we exposed 4 different crystal orientations: (100), $(1\bar{1}0)$, (111), and $(22\bar{1})$, to the interfaces and calculated the resulting NaCl solubility in water. We also added some defects to the crystal planes by randomly removing ions from the surface (keeping the system electroneutral) in order to help the system to exchange ions with the solution. Fig. 4 shows the solubility obtained for four crystal slabs of about the size of case E (2830 to 3034 ions in the crystal slab and 1620 water molecules) with different faces exposed to the solution at an initial concentration of about $4m$. As illustrated in Fig. 4, all the crystal orientations

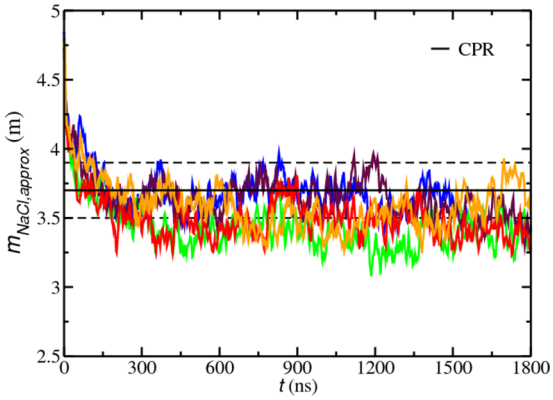

FIG. 3. Solution concentration as a function of time for 5 independent trajectories with different initial velocities corresponding to case E and exposing (100) plane to the interface. The water solution had an initial concentration of $4.75m$. Values were averaged over blocks of 8 ns to reduce high-frequency noise. Black lines indicate the value and error obtained from chemical potential routes.

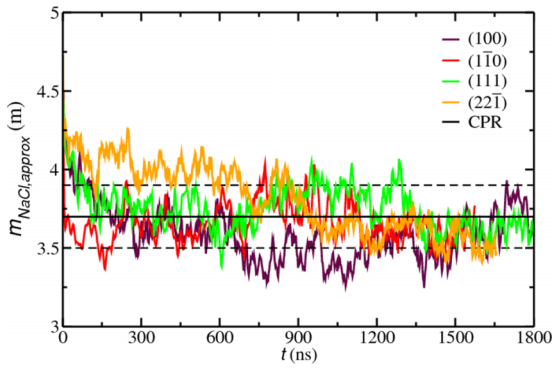

FIG. 4. Concentration of the solution as a function of time for several crystal planes as indicated in the legend. All the systems have a crystal slab consisting of 2830 to 3034 ions depending on the crystal orientation in contact with a water solution composed of 1620 molecules of water with an initial concentration of about $4m$. Values were averaged over blocks of 8 ns to reduce high-frequency noise. Black lines indicate the value and error obtained from chemical potential routes.

gave the same solubility, within the statistical noise analysed in Sec. III B. The average values of solubility obtained for the different crystal orientations were 3.5(4)m, 3.7(4)m, 3.8(4)m, and 3.7(4)m for (100), (1$\bar{1}$0), (111), and (22$\bar{1}$), respectively.

D. Dependence on the initial concentration of the solution

In order to reduce the computational cost for the system to reach equilibrium in direct coexistence simulations, it might be desirable to know whether adsorption or desorption of ions in the crystal slab is faster. Depending on such rates, it would be more computationally efficient to start from the supersaturated solutions or from the pure solvent. Although the time needed for a system to reach equilibrium may depend on the initial state of the simulation, different initial solution concentrations should eventually lead to the same solubility. To study the effect of the initial solution concentration on simulation efficiency and salt solubility, we prepared the crystal slab corresponding to case E with (1$\bar{1}$0) crystal orientation and put it in contact with pure water. We also prepared a crystal slab (case E) exposing the (22$\bar{1}$) crystal orientation to the interface in contact with three different solutions with concentrations of 4.6m, 4.9m, and 5.2m. To accelerate the exchange of ions between the solution and the crystal slab, some ions were removed from the crystal layers in contact with the solution generating interfacial defects. This turned out to be a crucial issue because in Ref. 21 no ions were dissolved in 500 ns in direct coexistence simulations using a defect-free crystal slab composed of 500 NaCl in contact with pure water with the (100) plane exposed to the interface. In the supplementary material, we provide some initial configurations of our runs as examples of configurations with interfacial defects. Additionally, the time required to reach the equilibrium concentration in other systems could be different for other NaCl/water models than that studied here (JC-SPC/E water model). Fig. 5 shows the evolution of the salt concentration as a function of time for these four simulations. The simulation started from 4.6m converged to equilibrium relatively quickly, while the ones starting from a solution of concentration 4.9m and from pure water converged after 750 ns and 1 μs, respectively. However, the simulation starting from an initial concentration of 5.2m reaches equilibrium only after 1700 ns. We have visually inspected how ions from initial supersaturated solutions (e.g., 4.6m, 4.9m, and 5.2m) were deposited on the interface of the crystal slab as the concentration of the solution decreased, and we observed that ions were placed at the crystal lattice positions. In principle, it seems difficult to determine if it is faster to reach the equilibrium concentration from a lower concentration or a higher one since stochasticity affects the time needed to reach equilibrium. Although the influence of initial solution concentration on simulation efficiency is not clear, all simulations starting from different initial salt concentrations reach similar solubility (around 3.7m), which is consistent with the CPR calculations.

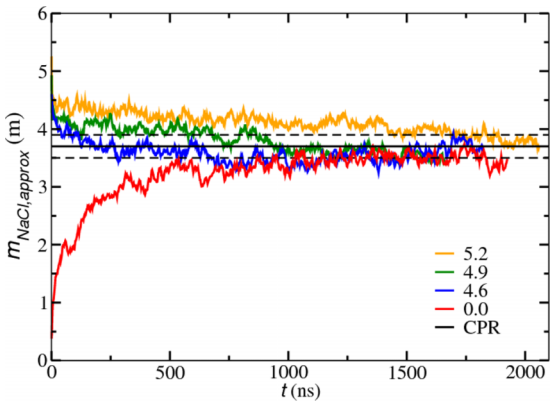

FIG. 5. Solution concentration as a function of time for a crystal slab consisting of about 2880 ions in contact with a solution of 1620 water molecules with different initial concentrations indicated in the legend. The crystal orientation of the NaCl slab at the interface was (1$\bar{1}$0) for the simulation starting from pure water and (22$\bar{1}$) for the cases starting from supersaturated solutions. Values were averaged over blocks of 8 ns to reduce high-frequency noise. Black lines indicate the value and error obtained from chemical potential routes.

IV. LJ BINARY MIXTURE

For the Lennard-Jones binary mixture, we simulated three different system sizes, as shown in Table III. All of the systems consisted of a solid and liquid slab with the same interfacial area, but different slab heights. The simulations were run for 1 μs, and data were collected after equilibration, usually about 50-100 ns into the simulation. Uncertainties were estimated by running ten simulations with different initial momenta for each system size. Unlike NaCl in water, the statistical noise between trials was much less than the fluctuations within each run. The solubility was also evaluated from CPR calculations (see the supplementary material for further details).

The dependence of the solubility on the width of the solid slab is shown in Fig. 6 and Table III. In contrast to NaCl in water, there is no change in the solubility with different size slabs, indicating minimal finite-size effects in the uncharged Lennard-Jones system. The direct coexistence method gives the same solubility as the chemical potential method.

The different system size effect in NaCl-water and binary LJ mixture may not be simply attributed to the presence of Coulombic interactions since no strong finite size effect was observed for DCM simulation of pure NaCl melts.[48] Therefore, we believe that a charged interface (shown in Fig. 7) in the

TABLE III. The number of solute particles in the crystalline slab N_S, the number of solvent particles in the solution N_{SV}, the width of the crystal slab L_{slab} (diameter in the case of the spherical crystallite), the area of the interface A_{int} and the solubility, expressed in mole fraction. In every case the initial solution concentration was 0.1 mole fraction.

Name	N_S	N_{SV}	L_{slab} (nm)	A_{int} (nm^2)	Solubility
CPR					0.036(2)
A	256	450	2.17	4.7	0.037(4)
B	384	675	3.25	4.7	0.037(3)
C	512	900	4.34	4.7	0.036(3)
SC	4537	9668	7.0		0.061(8)

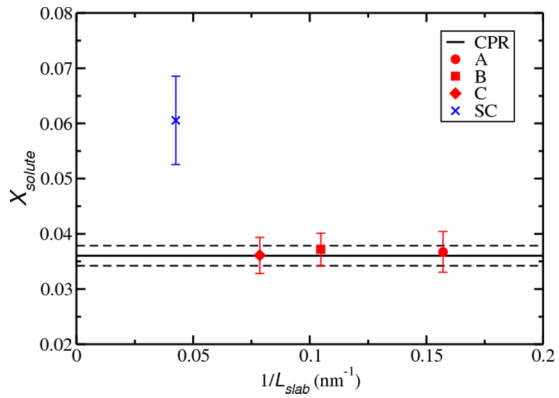

FIG. 6. Solubility in the binary LJ mixture for all system sizes studied as a function of the inverse width of the crystal slab. Red symbols indicate the calculated solubility using the direct coexistence method at different solid slab widths always exposing the (100) plane to the interfaces. The black lines indicate the value and error obtained from the chemical potential method extrapolated to infinite system size. The spherical crystallite (SC) value (explained in Sec. V and the supplementary material) has been plotted taking the inverse of its diameter (1/D) as the characteristic reciprocal length.

NaCl-water system is a possible cause of the strong finite size effect.

The formation of charged interfaces that give rise to dipoles may be due to the adsorption and desorption of ions at the interfaces. Fig. 7 shows the charge profile associated with the (100) crystal plane, see the supplementary material for the corresponding charge density profiles associated with different crystalline planes. Since the dielectric permittivity is much lower in the crystal than in solution, the dipoles might stress the structure of the crystal slab when the distance between both dipoles is short (i.e., less than 4 nm). This stress in the solid phase could increase the free energy of the solid (as shown in Ref. 49) and could cause the higher solubility that has been observed when the width of the crystal slabs is small.[21–23] Additionally, since Coulomb interactions decay slowly, a charge asymmetry at the interfaces could generate electric fields that will influence the energy (chemical potential) of the ions in the crystal bulk and, consequently, the calculated solubility.

Another issue that made it easier to obtain the solubility for the LJ binary mixture was that the kinetics of particle exchange between crystal and solution are faster compared to the ionic system, which is an interesting point that should be analyzed in more detail in future work. Most likely, the incorporation of a solute particle from the solution to the solid is an activated process (and the same is true for the process in which a solid particle passes to the solution). Since both ion-ion and ion-water interactions are much stronger than those found in the LJ system, one may expect larger free energy activation barriers for the solute exchange in the case of the NaCl system as compared to the LJ system, making the kinetics of particle exchange slower for ionic systems.

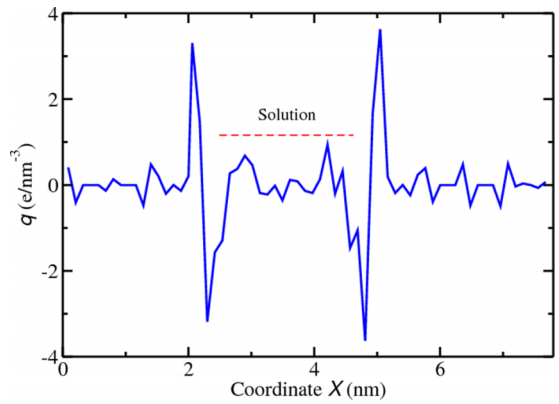

FIG. 7. Net ionic charge density profile obtained for the same NaCl crystal system as shown in Fig. 1(a). Partial charges of the water molecules were not considered in this plot.

V. SPHERICAL CRYSTALLITE FOR ESTIMATING SOLUBILITY

One variant of the DCM approach used to evaluate the solubility in recent work[23,24] is to insert a crystalline seed into a solution, an approach that has also been recently used to evaluate nucleation rates of salts from solution.[50] In this variant, instead of a slab geometry for both phases as in a standard direct coexistence simulation, a crystal cluster of ions is completely surrounded by a solution (or pure water). The concentration of the solution is evaluated after the system reaches equilibrium. In both publications,[23,24] the value obtained for the solubility of the JC/SPC/E model was about 5.8m, significantly higher than the values obtained from CPR calculations. In the present work, we also used this variant of DCM to calculate solubilities for the NaCl solution and the binary LJ mixture.

For the system of NaCl and water, a spherical NaCl crystal of 7230 ions (6 nm diameter) was inserted into a solution of 9200 water molecules with an initial concentration of 7.3m. For the LJ mixture, we inserted a crystal formed by 4540 solute particles (7 nm diameter) into a solution of 10 770 particles with an initial concentration of 0.1 mole fraction.

As shown in Fig. 2, the solubility of NaCl obtained from this simulation was 5.4m (further details in the supplementary material). This value is close to the ones obtained in Refs. 23 and 24 for JC-SPC/E models. By having a spherical crystal that is much larger than those used in prior simulations, we obtained slightly lower solubility than results reported in literature;[23,24] however, agreement with the CPR still cannot be reached. As shown in Fig. 6, for the binary LJ mixture the solubility obtained using the spherical crystal (SC) was 0.061(8) (mole fraction), which is significantly higher than those obtained by CPR and standard DCM calculations (0.036 mole fraction). Additionally, the uncertainty in the spherical crystal solubility is much larger than the other uncertainties since the simulations had a high computational cost and were only run for 200 ns. Therefore, it seems that this variant of DCM is not suitable for calculating solubility regardless of the system size or presence of charge.

We believe that the failure of this variant of DCM can be attributed to the Laplace pressure of the crystal, which increases the chemical potential of the solid. Since the chemical potential of the salt in the solution remains the same, the intersection of the chemical potential of the salt in the solution and that of the solid would take place at higher concentrations, resulting in apparently greater solubility. An

equivalent argument can be made from nucleation theory, namely, that the critical nucleus size, at which a crystal neither shrinks nor grows on average, depends on supersaturation, approaching infinite size at the solubility limit. The converse of this argument is that a crystal of finite size appears to be at equilibrium with a concentration higher than the equilibrium concentration. Therefore, in order to reach the solubility limit, an infinite spherical cluster having a flat interface would be needed.

VI. SUMMARY

The effects of size and geometry of the crystalline solid, statistical noise, crystal orientation, and initial solution concentration on the calculation of solubility for the NaCl-water system and the binary LJ mixture using DCM simulations were investigated. For NaCl in water, the calculated solubility was found to be independent of the crystal orientation and initial concentration within the stochastic uncertainty of about $0.3m$. It was found that the geometry of the solid, i.e., the width of the crystal slab, significantly affects the calculated solubility, and the DCM simulations yield consistent results with CPR calculations when the width of the NaCl crystal is above 4 nm. For the LJ binary mixture, we did not observe any comparable system-size effects on the solubility calculation. The strong finite-size effect in the NaCl-water system is possibly induced by charged interfaces between the solution and the crystalline solid. This hypothesis merits further detailed investigation.

We also tried one variant of DCM by inserting a spherical crystal into solution. For both NaCl in water and the binary LJ mixture, the solubility obtained by this method is higher than the value obtained by standard DCM and CPR. The failure of this method cannot be attributed to the finite size effect and is not related to the Coulombic interactions since the LJ mixture displays the same effect. We believe that these discrepancies may be due to a Laplace pressure effect. This, too, deserves further detailed investigation.

SUPPLEMENTARY MATERIAL

See supplementary material for details of our calculations for the solubility of the LJ binary mixture estimated by thermodynamic integration and also the calculated solubilities by inserting the spherical clusters in both systems (LJ and NaCl/water). Additionally, we show the net ionic density charge profiles for the different crystal orientations studied in the NaCl/water system. We also provide 3 different initial configurations with their corresponding files needed to be run in GROMACS (topology and input files for the simulation).

ACKNOWLEDGMENTS

Financial support for this work was provided by the Office of Basic Energy Sciences, U.S. Department of Energy, under Award No. DE-SC0002128. J. R. Espinosa acknowledges financial support from FPI Grant No. BES-2014-067625 and Project No. FIS2013-43209-P.

[1]T. Koop, B. Luo, A. Tsias, and T. Peter, Nature **406**, 611 (2000).
[2]E. Waisman and J. L. Lebowitz, J. Chem. Phys. **52**, 4037 (1970).
[3]L. L. Lee, *Molecular Thermodynamics of Electrolyte Solutions* (World Scientific, Singapore, 2008).
[4]D. Levesque, J. J. Weis, and G. N. Patey, J. Chem. Phys. **72**, 1887 (1980).
[5]L. Blum, Mol. Phys. **30**, 1529 (1975).
[6]I. S. Joung and T. E. Cheatham, J. Phys. Chem. B **113**, 9020 (2009).
[7]D. E. Smith and L. X. Dang, J. Chem. Phys. **100**, 3757 (1994).
[8]S. Weeransinghe and P. E. Smith, J. Chem. Phys. **119**, 11342 (2003).
[9]I. Nezbeda, F. Moucka, and W. R. Smith, J. Chem. Theory Comput. **9**, 5076 (2013).
[10]P. T. Kiss and A. Baranyai, J. Chem. Phys. **141**, 114501 (2014).
[11]I. Nezbeda, F. Moucka, and W. R. Smith, Mol. Phys. **114**, 1665 (2016).
[12]P. Cohen, *ASME Handbook on Water Technology for Thermal Power Systems* (ASME, New York, 1989).
[13]J. R. Espinosa, E. Sanz, C. Valeriani, and C. Vega, J. Chem. Phys. **139**, 144502 (2013).
[14]D. Rozmanov and P. G. Kusalik, Phys. Chem. Chem. Phys. **13**, 15501 (2011).
[15]V. C. Weiss, M. Rullich, C. Köhler, and T. Frauenheim, J. Chem. Phys. **135**, 034701 (2011).
[16]E. G. Noya, C. Vega, and E. de Miguel, J. Chem. Phys. **128**, 154507 (2008).
[17]J. R. Morris and X. Song, J. Chem. Phys. **116**, 9352 (2002).
[18]V. K. Michalis, J. Costandy, I. N. Tsimpanogiannis, A. K. Stubos, and I. G. Economou, J. Chem. Phys. **142**, 044501 (2015).
[19]D. G. Salgado and C. Vega, J. Chem. Phys. **132**, 094505 (2010).
[20]M. M. Conde and C. Vega, J. Chem. Phys. **133**, 064507 (2010).
[21]J. L. Aragones, E. Sanz, and C. Vega, J. Chem. Phys. **136**, 244508 (2012).
[22]K. Kobayashi, Y. Liang, T. Sakka, and T. Matsuoka, J. Chem. Phys. **140**, 144705 (2014).
[23]H. M. Manzanilla-Granados, H. Saint-Martin, R. Fuentes-Azcatl, and J. Alejandre, J. Phys. Chem. B **119**, 8389 (2015).
[24]H. Wiebe, J. Louwersheimer, and N. Weinberg, Mol. Phys. **113**, 3176 (2015).
[25]F. Moucka, I. Nezbeda, and W. R. Smith, J. Phys. Chem. B **138**, 154102 (2013).
[26]A. S. Paluch, S. Jayaraman, J. K. Shah, and E. J. Maginn, J. Chem. Phys. **133**, 124504 (2010).
[27]Z. Mester and A. Z. Panagiotopoulos, J. Chem. Phys. **142**, 044507 (2015).
[28]A. L. Benavides, J. L. Aragones, and C. Vega, J. Chem. Phys. **144**, 124504 (2016).
[29]E. Sanz and C. Vega, J. Chem. Phys. **126**, 014507 (2007).
[30]F. Moucka, I. Nezbeda, and W. R. Smith, J. Chem. Theory Comput. **11**, 1756 (2015).
[31]H. Jiang, Z. Mester, O. A. Moultos, I. G. Economu, and A. Z. Panagiotopoulos, J. Chem. Theory Comput. **11**, 3802 (2015).
[32]Z. Mester and A. Z. Panagiotopoulos, J. Chem. Phys. **143**, 044505 (2015).
[33]H. J. C. Berendsen, J. R. Grigera, and T. P. Straatsma, J. Phys. Chem. **91**, 6269 (1987).
[34]H. E. A. Huitema, B. van Hengstum, and J. P. van der Eerden, J. Chem. Phys. **111**, 10248 (1999).
[35]E. Lindahl, B. Hess, and D. van der Spoel, J. Mol. Model. **7**, 306 (2001).
[36]M. Parrinello and A. Rahman, J. App. Phys. **52**, 7182 (1981).
[37]S. Nosé, Mol. Phys. **52**, 255 (1984).
[38]U. Essmann, L. Perera, M. L. Berkowitz, T. Darden, H. Lee, and L. G. Pedersen, J. Chem. Phys. **103**, 8577 (1995).
[39]B. Hess, H. Bekker, H. J. C. Berendsen, and J. G. E. M. Fraaije, J. Comput. Chem. **18**, 1463 (1997).
[40]P. R. ten Wolde, M. J. Ruiz-Montero, and D. Frenkel, Faraday Discuss. **104**, 93 (1996).
[41]C. Valeriani, E. Sanz, and D. Frenkel, J. Chem. Phys. **122**, 194501 (2005).
[42]J. R. Espinosa, C. Vega, C. Valeriani, and E. Sanz, J. Chem. Phys. **142**, 194709 (2015).
[43]H. J. C. Berendsen and W. F. van Gunsteren, in *Molecular Liquids: Dynamics and Interactions*, edited by W. J. O.-T. A. J. Barnes and J. Yarwood (D. Reidel Publishing Company, 1984), p. 475.
[44]E. B. Moore and V. Molinero, Nature **479**, 506 (2011).
[45]L. Filion, R. Ni, D. Frenkel, and M. Dijkstra, J. Chem. Phys. **134**, 134901 (2011).
[46]J. Jover, A. J. Haslam, A. Galindo, G. Jackson, and E. A. Muller, J. Chem. Phys. **137**, 144505 (2012).
[47]J. Kolafa, paper presented at the 34th International Conference on Solution Chemistry, Czech Technical University, Prague, 2015.
[48]J. L. Aragones, C. Valeriani, E. Sanz, and C. Vega, J. Chem. Phys. **137**, 104507 (2012).
[49]E. G. Noya, M. M. Conde, and C. Vega, J. Chem. Phys. **129**, 104704 (2008).
[50]N. E. R. Zimmermann, B. Vorselaars, D. Quigley, and B. Peters, J. Am. Chem. Soc. **137**, 13352 (2015).